Chin. Phys. B Vol. 22, No. 10 (2013) 108402

The design and numerical analysis of tandem thermophotovoltaic cells*

Yang Hao-Yu(杨皓宇), Liu Ren-Jun(刘仁俊), Wang Lian-Kai(王连锴), Lü You(吕 游), Li Tian-Tian(李天天), Li Guo-Xing(李国兴), Zhang Yuan-Tao(张源涛)†, and Zhang Bao-Lin(张宝林)‡

State Key Laboratory on Integrated Optoelectronics, College of Electronic Science and Engineering, Jilin University, Changchun 130012, *China*

(Received 4 May 2013; revised manuscript received 6 June 2013)

In this paper, numerical analysis of GaSb ($E_g = 0.72$ eV)/$Ga_{0.84}In_{0.16}As_{0.14}Sb_{0.86}$ ($E_g = 0.53$ eV) tandem thermophotovoltaic (TPV) cells is carried out by using Silvaco/Atlas software. In the tandem cells, a GaSb p–n homojunction is used for the top cell and a GaInAsSb p–n homojunction for the bottom cell. A heavily doped GaSb tunnel junction connects the two sub-cells together. The simulations are carried out at a radiator temperature of 2000 K and a cell temperature of 300 K. The radiation photons are injected from the top of the tandem cells. Key properties of the single- and dual-junction TPV cells, including I–V characteristic, maximum output power (P_{max}), open-circuit voltage (V_{oc}), short-circuit current (I_{sc}), etc. are presented. The effects of the sub-cell thickness and carrier concentration on the key properties of tandem cells are investigated. A comparison of the dual-TPV cells with GaSb and GaInAsSb single junction cells shows that the P_{max} of tandem cells is almost twice as great as that of the single-junction cells.

Keywords: numerical simulation, GaSb-based compounds, tandem thermophotovoltaic cell, maximum output power

PACS: 84.60.Jt, 02.60.–x, 85.60.Bt, 71.55.Eq **DOI:** 10.1088/1674-1056/22/10/108402

1. Introduction

Thermophotovoltaic (TPV) cells based on the photovoltaic effect are of great importance for energy conversion devices in a temperature range of 1000 K–2000 K. III–V group semiconductors are suitable for TPV cells since their narrow direct band-gaps in a range from 0.3 eV to 0.7 eV closely match the peak wavelength of the thermal source.[1] Many III–V group semiconductors, such as GaSb, InGaAsSb, InGaAs, and InAsSbP, have been investigated for TPV applications. A comparison of fabrication techniques and characteristics among those TPV cells shows that GaSb-based TPV cells have obvious advantages in commercial applications.[2]

GaSb-based TPV cells have been developed for decades. For a two-step diffusion fabricated GaSb TPV, its V_{oc} is 0.45 V, and the fill factor (FF) is 0.72.[3–5] Quaternary InGaAsSb alloys can be achieved, which is lattice-matched to GaSb in an adjustable wide range of band-gap from 0.29 eV to 0.72 eV. GaInAsSb TPV cells have been successfully grown by metal–organic chemical vapor deposition (MOCVD)[5,6] and molecular beam epitaxy (MBE).[7,8] The external quantum efficiency (Q_{Eext}) is 65%, the FF is 0.67. There are two major methods to achieve high efficiency of TPV cells. One is to employ narrow direct band-gap materials as discussed above; the other is to use tandem TPV cells. Multi-junction structures are widely used in solar cells,[9] one of which has a high efficiency of 41.4%.[10] However, little work on GaSb–GaInAsSb tandem TPV cells has been reported, whose structure is similar to but not identical with that reported in this paper.[3,11–14] In this paper, monolithically stacked GaSb–GaInAsSb multi-junction TPV cell is designed and simulated. The characteristics of the GaSb–GaInAsSb tandem TPV cells, including I–V curve, P_{max}, V_{oc}, and I_{sc}, are analyzed and compared with those of single-junction TPV cells.

2. Method and structure

The tandem TPV structure consists of a GaSb p–n homojunction as the top cell, and a GaInAsSb p–n homojunction as the bottom cell. The two sub-cells are connected by a heavily doped GaSb tunnel junction. In order to improve P_{max}, the band-gap of the top cell is selected to be higher than that of the cell below it, as the wide spectrum photons can be absorbed efficiently. Figure 1 shows the cross-sectional structure of the single junction and the dual-junction TPV cells discussed in this paper. For the tandem structure, the GaInAsSb p–n homojunction, which is lattice-matched to GaSb, is fabricated on N-type GaSb substrate as the bottom cell. A heavily doped GaSb p–n homojunction as the tunnel junction is stacked on the GaInAsSb cell. The top cell is GaSb p–n homojunction with P-type ZnS ($E_g = 3.7$ eV) as the windows layer. The simulation is carried out at a radiator temperature of 2000 K and cell temperature of 300 K. The photons are injected from the top of each cell shown in Fig. 1.

*Project supported by the National Natural Science Foundation of China (Grant No. 61076010) and the Project of State Key Laboratory on Integrated Optoelectronics (Grant No. IOSKL2012ZZ13).

†Corresponding author. E-mail: zhangyt@jlu.edu.cn

‡Corresponding author. E-mail: zbl@jlu.edu.cn

© 2013 Chinese Physical Society and IOP Publishing Ltd

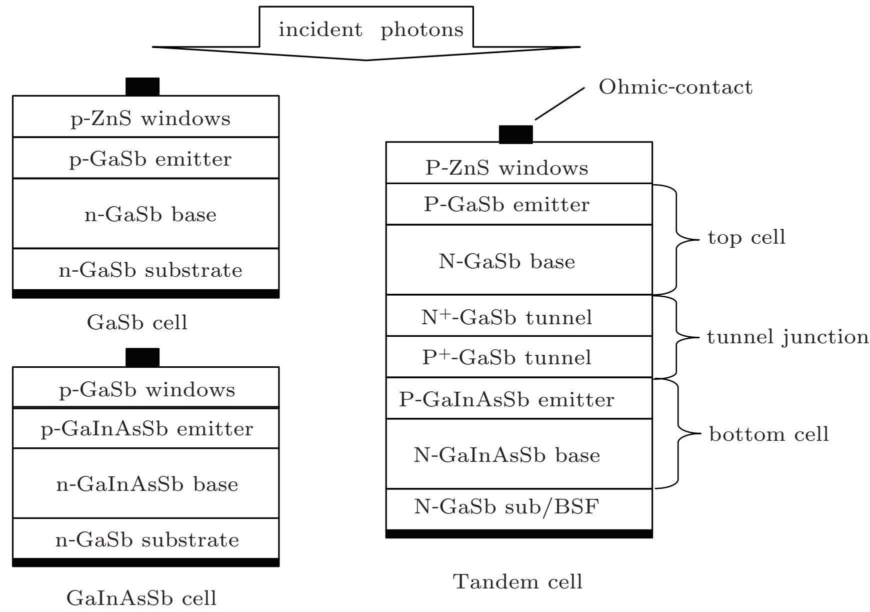

Fig. 1. Schematic cross sections of the simulated GaSb, GaInAsSb single TPV cell, and GaSb–GaInAsSb tandem TPV cell.

Table 1. Parameters of GaSb and $Ga_{0.84}In_{0.16}As_{0.14}Sb_{0.86}$ for the TPV cell simulation.

Parameters (300 K)	GaSb	$Ga_{0.84}In_{0.16}As_{0.14}Sb_{0.86}$
E_g/eV	0.726	0.532
N_c/cm^{-3}	5.44×10^{17}	1.7×10^{17}
N_v/cm^{-3}	4.78×10^{18}	5.3×10^{18}
ε	15.7	15.63
χ/eV	4.06	4.15
$(\mu_{max\cdot e}/\mu_{min\cdot e})$/cm$^2\cdot$V$^{-1}\cdot$s^{-1}	5650/1050	8920/610
$(\mu_{max\cdot h}/\mu_{min\cdot h})$/cm$^2\cdot$V$^{-1}\cdot$s^{-1}	875/190	420/110
τ_e/s	1×10^{-6}	1×10^{-7}
τ_h/s	1×10^{-6}	1×10^{-7}
B/cm$^3\cdot$s^{-1}	1.34×10^{-10}	5.5×10^{-11}
C_{Ae}/cm$^6\cdot$s^{-1}	4.19×10^{-29}	1.07×10^{-27}
C_{Ah}/cm$^6\cdot$s^{-1}	3.92×10^{-28}	2.15×10^{-28}

The simulation of the TPV cells is carried out by using the Atlas simulator from the Silvaco software package for optoelectronic devices.[15] Taking into account both accuracy and practicability, the Caughey–Thomas theory is chosen for the carrier concentration and temperature-dependent mobility model. SRH, Auger and surface recombination are chosen for the carrier recombination models. There are several models for tunnel junctions. The two main models are the band-to-band tunneling model and the non-local band-to-band tunneling model. The first model uses the electric field value at each node to give a generation rate at that point due to the tunneling. In reality, the tunneling process is non-local, and it is necessary to take into account the spatial profile of the energy bands. It is also necessary to take into account the spatial separation of the electrons generated in the conduction band from the holes generated in the valence band. Adachi's dispersion model is used for optical simulation. The accuracy of this simulation tool strongly depends on the accuracy of the material parameters used in constructing the above models.[16,17] The material parameters of the GaSb and GaInAsSb are summarized for the simulation in Table 1. Since the TPV cells have almost the same theory as solar cells, similar common approaches to the study of the tandem solar cell system are employed for the tandem TPV cells.[18,19]

3. Results and discussion

3.1. Comparison of the P–N structure with the N–P structure

The GaSb and GaInAsSb single-cells are first modeled and simulated individually. In this way, their structure (N–P junction or P–N junction) can be optimized and chosen. Figures 2 and 3 show the I–V curve of GaSb cell and GaInAsSb cell with different thickness values of emitter and base regions, respectively. P_{max} is also achieved and marked in Figs. 2 and 3. In Figs. 2(a) and 2(b), the thickness values of both base and emitter have little influence on V_{oc}. The main difference between the two structures is that P_{max} and I_{sc} of N–P structure are a little higher than those of the P–N structure. For the GaInAsSb N–P structure, region thickness has the same influence on P_{max} as the GaSb N–P structure. However, in the P–N structure, as the P-type region thickness (H_p) is much larger than N-type region thickness (H_n), it leads to higher I_{sc}, P_{max}, and smaller V_{oc} than those in the case of $H_p \ll H_n$. It indicates that if P-type GaInAsSb as the emitter in the P–N structure is the main photon absorption area, the efficiency of the photon-generated carriers and P_{max} could be raised. The minority carrier diffusion length ($L_{e,P}/L_{h,N}$) is an important parameter in determining the carrier collection efficiency.[20] In the P-type GaInAsSb, since the minority carrier mobility ($\mu_{e,P}$) is much higher than the majority carrier mobility ($\mu_{h,P}$), $L_{e,P} \gg L_{h,N}$. Thus, it is concluded that

P–N structure GaInAsSb TPV cells have higher P_{max} than N–P structure GaInAsSb TPV cells with the same emitter and base thickness, which is also proved in Fig. 3. In the following discussion, we mainly focus on tandem cells with the P–N structure.

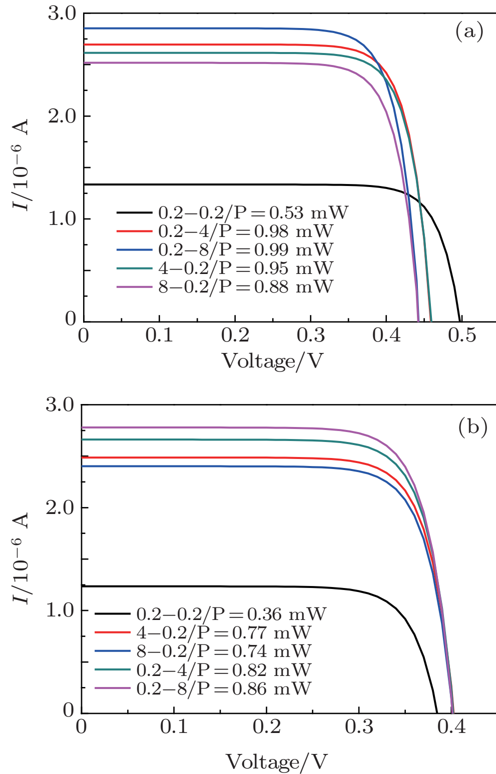

Fig. 2. (color online) (a) *I–V* curves of N–P GaSb TPV cell with different emitters and base thickness values; (b) *I–V* curve of P–N GaSb TPV cell with different emitters and base thickness values.

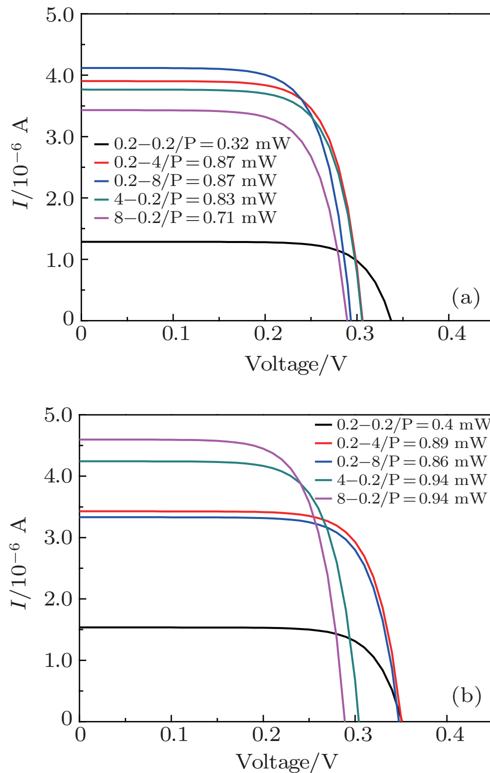

Fig. 3. (color online) (a) *I–V* curve of an N–P GaInAsSb TPV cell with different emitters and base thicknesses; (b) *I–V* curve of P–N GaInAsSb TPV cell with different emitters and base thickness values.

3.2. Effect of region thickness

In this section, different base and emitter thickness values in the top and bottom cells are simulated, respectively. P_{max}, V_{oc}, and I_{sc} of the tandem TPV cell are presented for a variety of thickness values.

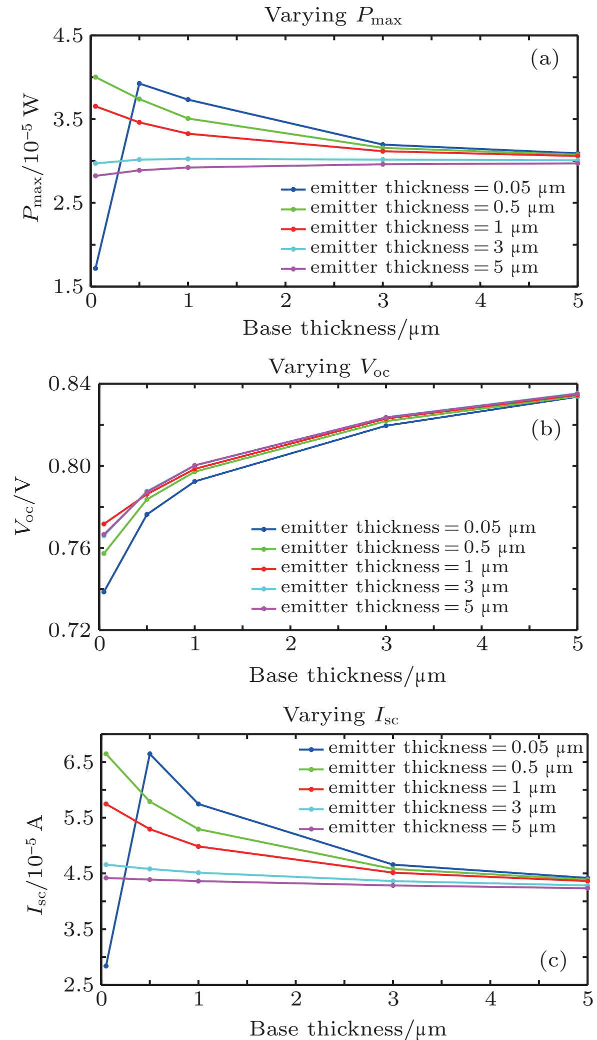

Fig. 4. (color online) Simulated (a) P_{max}, (b) V_{oc}, and (c) I_{sc} versus base thickness of top cell with a variety of emitter thickness values.

Figure 4 presents the effects of the emitter and base thickness parameters of the top cell on P_{max}, V_{oc}, and I_{sc}, respectively, with the other parameters listed in Table 1 kept unchanged. Figure 4 indicates that P_{max} of tandem cells is decreasing with both emitter and base thickness of top cell increasing. While the emitter thickness values are in a range of 3 μm to 5 μm, P_{max} almost stays constant. For an emitter thickness thinner than 3 μm, P_{max} increases rapidly with base thickness decreasing. The reason is that the region thickness of the top cell should be thick enough to ensure that more photons, which are not absorbed by the top cell, can reach the bot-

tom cell. However, there is a singularity in Fig. 4(a), where the base thickness and the emitter thickness are both 0.05 μm. As discussed in Subsection 3.1, the P-type region is the main photon absorption area. Therefore, increasing of the P-type region thickness is conducive to a higher collection efficiency of the photon-generated carriers. However, based on photovoltaic theory, the emitter thickness should be smaller than $L_{e,P}$ to obtain a high collection efficiency of the photon-generated carriers; meanwhile, emitter thickness should be thick enough to fully absorb the incident light.[21] The emitter thickness of 0.05 μm is not thick enough to absorb the incident photons, so the P_{max} decreases rapidly.

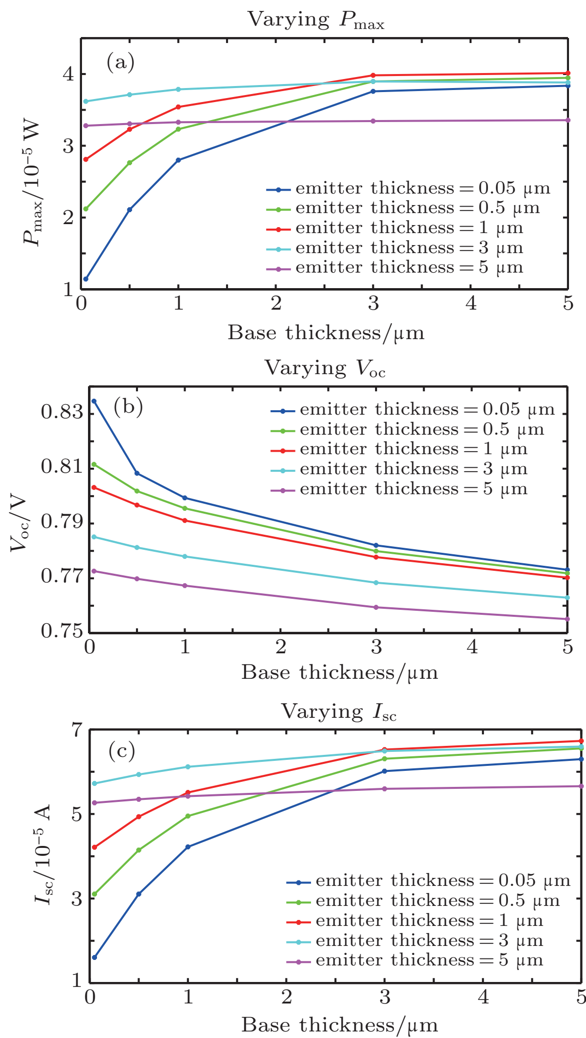

Fig. 5. (color online) Simulated (a) P_{max}, (b) V_{oc}, and (c) I_{sc} versus base thickness of bottom cell with a variety of emitter thickness values.

Figure 5 shows the effects of the emitter and base thickness of the bottom cell on P_{max}, V_{oc}, and I_{sc}, with other parameters from Table 1 fixed to be constant. It indicates that P_{max} increases with base thickness increasing. While the base thickness is higher than 3 μm, P_{max} almost stays constant. With emitter thickness increasing, P_{max} tends to increase first, and then decreases as shown in Fig. 5(a). P_{max} reaches its maximum value for the 3-μm-thick emitter of the bottom cell. The reason for the emitter thickness influencing P_{max} has been discussed above.

3.3. Effect of region carrier concentration

Figures 6 and 7 show the P_{max}, V_{oc}, and I_{sc} of the tandem cells for different emitter and base carrier concentrations of the top cell and the bottom cell, with other parameters listed in Table 1 keeping constant, respectively. For the top cell in Fig. 6, P_{max} decreases with the base carrier concentration increasing and the emitter carrier concentration decreasing separately. However, the base carrier concentration has a stronger influence on P_{max} than that of the emitter region. P_{max} is almost constant with the base carrier concentration varying from 1×10^{17} cm^{-3} to 6.3×10^{18} cm^{-3}. As the base carrier concentration increases above 6.3×10^{18} cm^{-3}, P_{max} rapidly decreases. For the bottom cell, P_{max} is almost not influenced by base carrier concentration, but strongly depends on emitter carrier concentration. With the emitter carrier concentration increasing, P_{max} declines overall. While the emitter carrier concentration is in a range from 10^{17} cm^{-3} to 10^{18} cm^{-3},

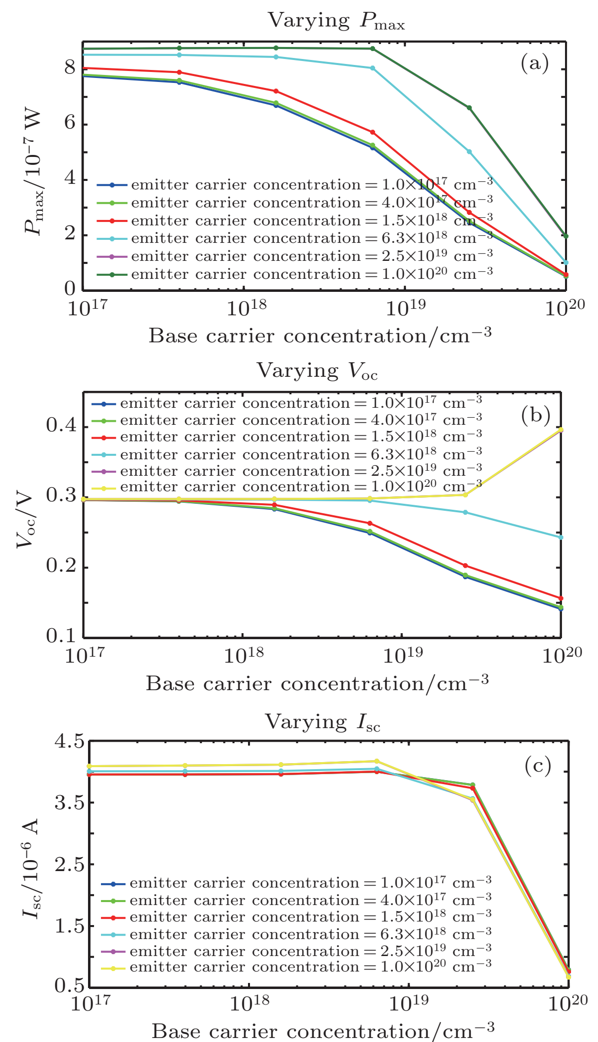

Fig. 6. (color online) Simulated (a) P_{max}, (b) V_{oc}, and (c) I_{sc} of tandem cells versus base carrier concentration for different emitter carrier concentrations of the top cell.

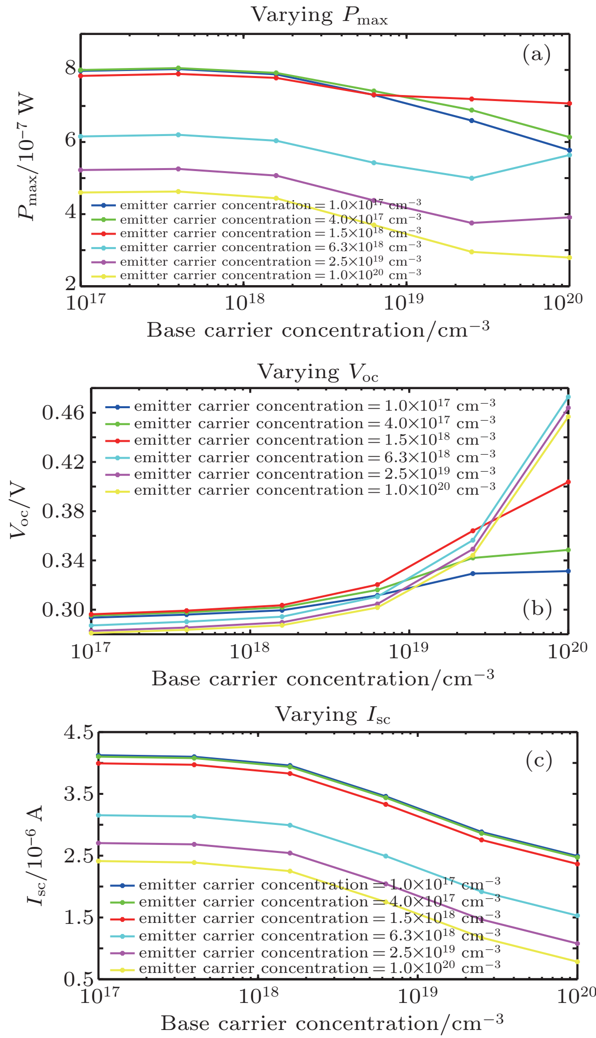

Fig. 7. (color online) Simulated (a) P_{max}, (b) V_{oc}, and (c) I_{sc} of tandem cells versus base carrier concentration for different emitter carrier concentrations of the bottom cell.

P_{max} is constant. As the emitter carrier concentration increases above 10^{18} cm^{-3}, P_{max} decreases rapidly. It indicates that the decrease of the emitter carrier concentration of the bottom cell improves $L_{e,P}$ and finally leads to the increase of P_{max}.

The tandem TPV cells are simulated with the optimized parameter listed in Table 2. The TPV cell area (W_{cell}) is 500 μm×500 μm. The radiation temperature (T_{rad}) is 2000 K, with the cell temperature (T_{cell}) of 300 K. Figure 8 shows the *I–V* curves of the tandem cells and the single-cells. Comparing with the seldom reported GaSb–GaInAsSb tandem TPV cells in Refs. [3] and [12], which acquire a maximal V_{oc} of 0.65 V; the V_{oc} of the GaSb–GaInAsSb tandem TPV cells we simulated is as high as 0.76 V. It proves that the structure of our tandem TPV cell is more advanced. The result shows that P_{max} of the tandem cells is 2.0 and 1.9 times those of the GaSb and the GaInAsSb cell, respectively.

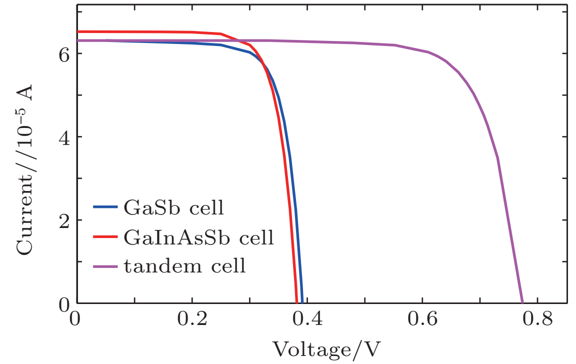

Fig. 8. (color online) *I–V* curves of the optimized tandem cells, the GaSb cell, and the GaInAsSb cell.

Table 2. Optimized tandem cell parameters for device simulation.

	W_{cell}=500 μm×500 μm, T_{rad} = 2000 K, T_{cell} = 300 K,					
	Top cell		Bottom cell			
	Emitter	Base	Emitter	Base	Windows	BSF
Thickness/μm	0.1	0.5	1	3	0.05	0.03
Concentration/cm^{-3}	1×10^{19}	1×10^{17}–5×10^{18}	1×10^{17}–1×10^{18}	1×10^{17}–1×10^{18}	1×10^{19}	1×10^{18}

4. Conclusions

In this paper, numerical analyses are performed for the GaSb TPV cell, the GaInAsSb TPV cell, and the GaSb–GaInAsSb tandem TPV cells, by using the two-dimensional numerical photovoltaic cell simulator Silvaco/Atlas. For the GaSb TPV cells, the P–N or N–P structures have a little effect on P_{max}. However, for the GaInAsSb TPV cell, the P–N structure presents a higher P_{max} than the N–P structure, since $\mu_{e,P}$ is much higher than $\mu_{h,P}$ in P-type GaInAsSb material. The tandem TPV cells consist of a GaSb homojunction as the top cell and a GaInAsSb homojunction as the bottom cell. Based on the simulation results, with emitter and base thickness of the top cell increasing, the P_{max} of the tandem cells decreases. For the bottom cell, the P_{max} increases rapidly as the base thickness of the bottom cell increases. However, when the base thickness increases above 3 μm, P_{max} is constant at a maximum value. For the effects of carrier concentration on P_{max} of the top cell and the bottom cell, with base carrier concentration increasing, P_{max} declines overall. In the top cell, P_{max} is somewhat influenced by the emitter carrier concentration, but it is strongly influenced by base carrier concentration. P_{max} decreases rapidly with base carrier concentration increasing. In the bottom cell, P_{max} is almost constant for a variety of base carrier concentrations. When the emitter carrier

concentration increases above 1×10^{18} cm^{-3}, $P_{\max}$ decreases rapidly. Simulating with device parameters fixed to be constant, $P_{\max}$ of the tandem TPV cell is almost 2 times that of the single-cells. For further improvements of the tandem cell performance, in order to increase the collection efficiency of the photon-generated carriers, wide band-gap lattice-matched window layers for GaSb and GaInAsSb cell and back-surface field cladding layers are considered to be applied to the tandem cell structures. The tunnel junction also needs to be optimized using different materials, such that it has a higher peak current, thereby reducing the current loss of tandem cells.

Acknowledgment

The authors are deeply grateful to Dr. Peng Xin-Cun and other members of the III–V Sb-based semiconductor group for useful discussions on simulation and optimization.

References

[1] Coutts T J and Ward J S 1999 *IEEE Trans. Electron. Dev.* **46** 2145
[2] Wang C A 2004 *Am. Inst. Phys. Conf. Proc.* **738** 255
[3] Mauk M G and Andreev V M 2003 *Semicond. Sci. Technol.* **18** S191
[4] Martin D and Algora C 2004 *Semicond. Sci. Technol.* **19** 1040
[5] Wang C A, Huang R K, Shiau D A, Connors M K, Murphy P G, O'Brien P W and Anderson A C M 2003 *Appl. Phys. Lett.* **83** 1286
[6] Welser E, Dimroth F, Ohm A, Guter W, Siefer G, Pholipps S, Schöne J, Polychroniadis E K, Konidaris S and Bett A W 2007 *Am. Inst. Phys. Conf. Proc.* **890** 107
[7] Bi W G and Li A Z 1992 *Chin. Phys. Lett.* **9** 325
[8] Bi W G and Li A Z 1992 *Chin. Phys. Lett.* **9** 53
[9] Mathieu, Baudrit and Carlos Algora 2010 *Phys. Status Solidi A* **207** 474
[10] FhG press release, 2010 www.ise.fraunhofer.de.
[11] Wilt D M, Wehrer R J, Maurer W F, Jenkins P P, Wernsman B and Schultz R W 2004 *Am. Inst. Phys. Conf. Proc.* **738** 453
[12] Andreev V M, Khvostikov V P, Rumyantsev V D, Sorokina S V and Shvarts M Z 2000 *Proceedings of the* 28*th IEEE Photovoltaic Specialists Conference*, September 15–22, 2000, Anchorage, USA, p. 1265
[13] Wanlass M W and Albin D S 2004 *Am. Inst. Phys. Conf. Proc.* **738** 462
[14] Siergiej R R, Sinharoy S, Valko T, Wehrer R J, Wernsman B, Link S D, Schultz R W and Messham R L 2004 *Am. Inst. Phys. Conf. Proc.* **738** 480
[15] ATLAS User's Manual. 2010 *Silvaco International* 2
[16] Gonzsalez-Cuevas J A, Refaat T F, Abedin M M and Elsayed Ali H E 2007 *J. Appl. Phys.* **102** 014504
[17] Muňoz M, Wei K, Pollak F H, Freeouf J L, Wang C A and Charache G W 2000 *J. Appl. Phys.* **87** 1780
[18] Lei Q S, Wu Z M, Geng X H, Zhao Y, Sun J and Xi J P 2006 *Chin. Phys.* **15** 3033
[19] Gao Xin, Yang S S, Xue Y X, Li K, Li D M, Wang Y, Wang Y F and Feng Z Z 2009 *Chin. Phys. B* **18** 5015
[20] Peng X C, Guo X, Zhang B L, Li X P, Zhao X W, Dong X, Zheng W and Du G T 2009 *Infrared Phys. Technol.* **52** 152
[21] Sze S M 1999 *Physics of Semiconductor Devices*, 2nd edn. (New York: Wiley) p. 575